American Mineralogist, Volume 61, pages 626–637, 1976

Clinopyroxene geothermometry of spinel-lherzolites

CLAUDE T. HERZBERG

Department of Geology, University of Western Ontario
London, Ontario, Canada N6A 5B7

AND NEIL A. CHAPMAN

Department of Earth Sciences, University of Leeds
Leeds, England LS2 9JT

Abstract

Experiments in the system $CaO–MgO–Al_2O_3–SiO_2$ have shown that the calcium tschermak's molecule ($CaAl_2SiO_6$) content of clinopyroxene in the spinel–lherzolite assemblage (forsterite + clinopyroxene + orthopyroxene + spinel) varies sympathetically with the $MgSiO_3$ content with changes in temperatures and pressure. Such variations are predominantly temperature-dependent, although both pyroxene end-members decrease slightly in amount with increases in pressure at constant temperature. Contrary to O'Hara (1967), the isopleths of $CaAl_2SiO_6$ and $MgSiO_3$ of clinopyroxene in temperature–pressure space are parallel, rendering these two pyroxene molecules indicators only of the temperature of equilibrium of spinel–lherzolites. No information on the pressures of equilibrium can be obtained.

Using simple thermodynamic mixing models of the solid solution phases participating in the subsolidus exchange reactions, two temperature estimations can be made of natural spinel–lherzolites from the experimental data of the synthetic system. The first temperature estimation is based on the equilibrium exchange of $Mg_2Si_2O_6$ between clinopyroxene and orthopyroxene at 12 kbar (equilibrium constant K_1) and the second temperature estimation is based on the equilibrium exchange of $CaAl_2SiO_6$ between clinopyroxene, olivine, and spinel at 12 kbar (equilibrium constant K_2).

Two temperature estimations were made from each of the analyses of the coexisting minerals of spinel–lherzolites from alpine-type intrusions and nodules in basalt (analyses obtained from the literature). The estimated temperatures for the spinel–lherzolite nodules in basalt range from the water-undersaturated peridotite solidus to the anhydrous solidus, indicating a close genetic relationship with the host basalts or those of the same fractionation suite. The temperatures estimated for most spinel–lherzolite intrusions indicate solidus temperatures followed by a cooling history of partial reequilibration to subsolidus temperatures. These temperatures probably bear little, if any, relationship to those of a normal geothermal gradient.

Introduction

Advances made in the experimental study of pyroxene solid-solution equilibria during the last decade have recently revived an interest in the direct measurement of paleogeothermal regimes in the upper mantle. Estimations of the paleogeothermal gradient beneath South Africa (Boyd, 1973; Boyd and Nixon, 1973) and the Norwegian Caledonides (Carswell, 1974), based on the enstatite and alumina solubility of pyroxenes in garnet–lherzolites, will undoubtedly be modified as experimental data become more refined; however, it is unlikely that they will depart significantly from the normal shield geotherms as originally defined by Ringwood (1966).

More recently similar attempts at determining paleogeothermal gradients at higher upper-mantle levels have been made from pyroxene geothermometry and geobarometry of spinel–lherzolites (MacGregor, 1974; MacGregor and Basu, 1974). It is the purpose of this work to reevaluate these estimates on the basis of new experimental results

on clinopyroxene solid solution geothermometry and geobarometry of spinel–lherzolites in the system $CaO–MgO–Al_2O_3–SiO_2$.

The immediate problem encountered in the pursuit of this task involves applying experimental data on synthetic systems to the chemistry of the natural peridotite system. Experimental data on the join $Mg_2Si_2O_6–CaMgSi_2O_6$ at 30 kbar (Davis and Boyd, 1966) have conventionally been used as the geothermometer and the alumina content of enstatite in the system $MgO–Al_2O_3–SiO_2$ (MacGregor, 1974) as the geobarometer for determining upper mantle geotherms (Boyd, 1973; Boyd and Nixon, 1973). The 1600°C and 30 kbar data of O'Hara and Schairer (1963), however, indicate that significant amounts of Al^{+3} in the pyroxene phases may appreciably effect the solubility of $Mg_2Si_2O_6$ in clinopyroxene. O'Hara (1967) later emphasized the necessity for advancing from simple two-pyroxene end-member systems of three components to three-pyroxene end-member systems of four components involving $CaO–MgO–Al_2O_3–SiO_2$ in order to adequately represent the major reaction relationships of four-phase lherzolites.

The task of this experimental work has been to investigate the change in the solubility of both $CaAl_2SiO_6$ and $MgSiO_3$ in clinopyroxenes of the spinel–lherzolite assemblage (forsterite + clinopyroxene + orthopyroxene + spinel) in the system $CaO–MgO–Al_2O_3–SiO_2$ with changes in temperature and pressure. In order to apply these experimental results to natural spinel–lherzolites, simple thermodynamic models, similar to those of Wood and Banno (1973), were constructed. These models enable the temperatures of equilbration of spinel–lherzolites to be estimated, providing that the compositions of all four phases are known. Wood (1974) later demonstrated experimentally the validity of these simple models in correcting for the presence of the components of the natural system not used in the experiments.

Experimental and analytical methods

All experiments were carried out using a single-stage, half-inch piston-cylinder apparatus similar to that described by O'Hara *et al.* (1971). The piston-out technique, as described by Richardson *et al.* (1968), was used with an over-pressure of 5 kbar. No friction correction was made to the nominal pressures reported in the tables and figures. The furnace cell was similar to that used by Richardson *et al.*, but without the ceramic disc between the thermocouple tip and capsule, and with the lower pyrophyllite spacer replaced by ceramic. Pt/Pt13Rh thermocouples were used to measure and control the temperatures of the furnace cell. Pressure-uncorrected temperatures were recorded and are presented in the tables and figures.

The compositions used in these experiments were:

AF = anorthite ($CaAl_2Si_2O_8$) + forsterite (Mg_2SiO_4) gel crystallized at 1200°C for 28 days at atmospheric pressure (<0.10 μm grain size).

A3F = anorthite ($CaAl_2Si_2O_8$) + 3 forsterite (Mg_2SiO_4) gel crystallized as above.

GP = anorthite ($CaAl_2Si_2O_8$) + 3 forsterite (Mg_2SiO_4) + diopside ($CaMgSi_2O_6$) + enstatite (Mg_2SiO_6) gel crystallized as above.

For experiments at temperatures near the solidus the charges were dried in order to avoid partial melting. For low-temperature experiments the charge was either left undried or it was dampened with a minor quantity of distilled water (<0.1 wt%) in order to flux the reaction and promote crystal growth. The drying technique used for each experiment is listed with the results in Table 1.

The experimental charges after the runs usually contained individual crystal sizes of less than 3 to 4 microns, whether or not trace amounts of water were used to promote crystal growth. Individual clinopyroxene crystals were commonly intergrown with orthopyroxene and spinel. Because of these textural complications, due to the nature of the finely crystalline starting materials, electron microprobe analyses of the clinopyroxenes proved too inaccurate to be of value. Consequently an X-ray diffraction method was developed in order to determine the amount of $MgSiO_3$ and $CaAl_2SiO_6$ in the clinopyroxene. This experimental method was used in preference to the traditional method of synthesis from glass starting materials (which usually produces crystals big enough to analyze by the electron microprobe) in order to minimize the possibility of synthesizing highly disordered metastable pyroxenes (Biggar and O'Hara, 1969; Howells and O'Hara, 1975).

The cell dimensions of the $CaMgSi_2O_6–MgSiO_3–CaAl_2SiO_6$ solid solution series vary with composition (Clark *et al.*, 1962). From these cell dimensions, the clinopyroxene CuKα $22\bar{1}$ and 310 diffraction angles were calculated; these are presented in Figure 1 by broken lines. The grid shown by the broken lines was then adjusted to the diffraction angles of three synthesized clinopyroxenes whose compositions are indicated by the solid lines. The goniometer

TABLE 1. Experimental results

Starting Material	Temperature °C	Pressure kbar	Time hours	Drying Procedure	Phase Identification	°2θ CuK$_\alpha$ Cpx 22$\bar{1}$	°2θ CuK$_\alpha$ Cpx 310	Wt % $CaAl_2SiO_6$ in Cpx	Wt % $MgSiO_3$ in Cpx
GP	1100	12.0	20.0	iii-b	Fo,Cpx,Opx,Sp	29.887 ±.003	30.411 ±.005	10.5	7.3
GP	1100	17.9	21.0	iii-b	Fo,Cpx,Opx,Sp,An*	29.883 ±.006	30.384 ±.020	9.2	5.7
GP	1100	18.0	20.1	iii-b	Fo,Cpx,Opx,Sp	20.878 ±.004	30.380 ±.005	8.6	6.5
GP	1200	12.0	18.2	i-a	Fo,Cpx,Opx,Sp	29.902 ±.002	30.472 ±.004	15.5	10.8
AF	1200	8.9	18.5	i-a	Fo,Cpx,Opx,Sp,An	29.904 ±.002	30.486 ±.005	17.1	11.6
GP	1200	18.0	18.1	i-a	Fo,Cpx,Opx,Sp	29.895 ±.003	30.443 ±.005	13.6	9.3
A3F	1270	10.0	19.5	i-a	Fo,Cpx,Opx,Sp	29.913 ±.005	30.557 ±.006	21.4	16.2
A3F	1270	11.2	18.5	i-a	Fo,Cpx,Opx,Sp	29.913 ±.004	30.537 ±.004	20.6	15.0
A3F	1270	12.9	18.7	i-a	Fo,Cpx,Opx,Sp	29.910 ±.004	30.522 ±.006	19.4	13.9
A3F	1300	14.0	18.0	i-a	Fo,Cpx,Opx,Sp	29.914 ±.003	30.545 ±.007	20.8	15.6
A3F	1300	16.2	18.3	i-a	Fo,Cpx,Opx,Sp	29.910 ±.002	30.525 ±.004	19.7	14.1
A3F	1300	17.0	19.8	i-a	Fo,Cpx,Opx,Sp	29.910 ±.002	30.517 ±.003	19.2	13.6
GP	1300	16.0	18.2	i-a	Fo,Cpx,Opx,Sp	29.911 ±.003	30.525 ±.004	19.8	14.3
A3F	1400	20.0	18.0	i-a	Fo,Cpx,Opx,Sp	29.915 ±.005	30.594 ±.006	23.6	19.5
A3F	1400	21.0	18.2	i-a	Fo,Cpx,Opx,Sp	29.915 ±.004	30.586 ±.004	23.1	18.9

i = charge dried in unsealed Pt tube at 1100°C for one hour prior to sealing.
iii = charge dampened with H_2O and Pt tube left unsealed. a = furnace cell dried in nitrogen furnace 0.5 hour at 800°C. b = furnace cell left undried. * = trace. Fo = forsterite. Cpx = clinopyroxene. Opx = orthopyroxene. Sp = spinel. An = anorthite.

was allowed to oscillate 8 to 10 times at a scan speed of 1/4° 2Θ per minute across the clinopyroxene diffraction peaks as well as the standard sodium chloride 200 diffraction angle (31.718° 2Θ). Sharp and well-defined diffraction peaks and a variation about the mean of ± 0.004° 2Θ indicated chemical homogeneity of the synthesized clinopyroxenes. A comparison of X-ray diffraction data from Clark *et al.* (1962) and Biggar (1969) with Figure 1 (solid lines) indicates an interlaboratory agreement of ± 3 weight percent $CaAl_2SiO_6$ and ± 2 weight percent $MgSiO_3$ in the determination of a stoichiometric clinopyroxene composition.

All experimental charges were inspected optically and by X-ray diffraction for glass and metastable phases. Nickel-filtered CuKα radiation generated at 28 mA and 44 kV from a Philips machine was used. A 0.2 mm receiving slit, a 4° scatter slit, and a 1° divergence slit were used. A small quantity of laboratory sodium chloride was mixed with each run product as an X-ray internal standard. From the mean clinopyroxene 22$\bar{1}$ and 310 diffraction angles, measured to 0.002° 2Θ for each oscillation, and Figure 1 (solid lines), the composition of the clinopyroxene synthesized with forsterite, orthopyroxene, and spinel was obtained. This composition was assumed to be stoichiometric with respect to $CaAl_2SiO_6$ and $Mg_2Si_2O_6$, or the chemically equivalent end-members $CaMgSi_2O_6$–$MgAl_2SiO_6$.

Discussion of results

The experimental results are listed in Table 1. The clinopyroxene 22$\bar{1}$ and 310 X-ray diffraction angles for each experiment were plotted on the X-ray diffraction-composition grid of Figure 1 and are shown in Figure 2. All the measurements plot along a common curve. From Figure 2 the $CaAl_2SiO_6$ and $MgSiO_3$ contents of clinopyroxene for each experiment were obtained, and these are shown in Figure 3.

Thirteen runs on A3F at 1100°C and 1200°C (not shown in Figure 3) were rejected due to the presence of incompletely reacted anorthite coexisting with the spinel–lherzolite phase assemblage. Excess anorthite in these charges resulted in anomalously high $CaAl_2SiO_6$ and $MgSiO_3$ contents of the clinopyroxenes. In order for the phase rule to be satisfied, only those charges which were anorthite-free were accepted as possibly representing equilibrium products. We have no proof that these data are equilibrium results, and know of no method whereby equilibrium

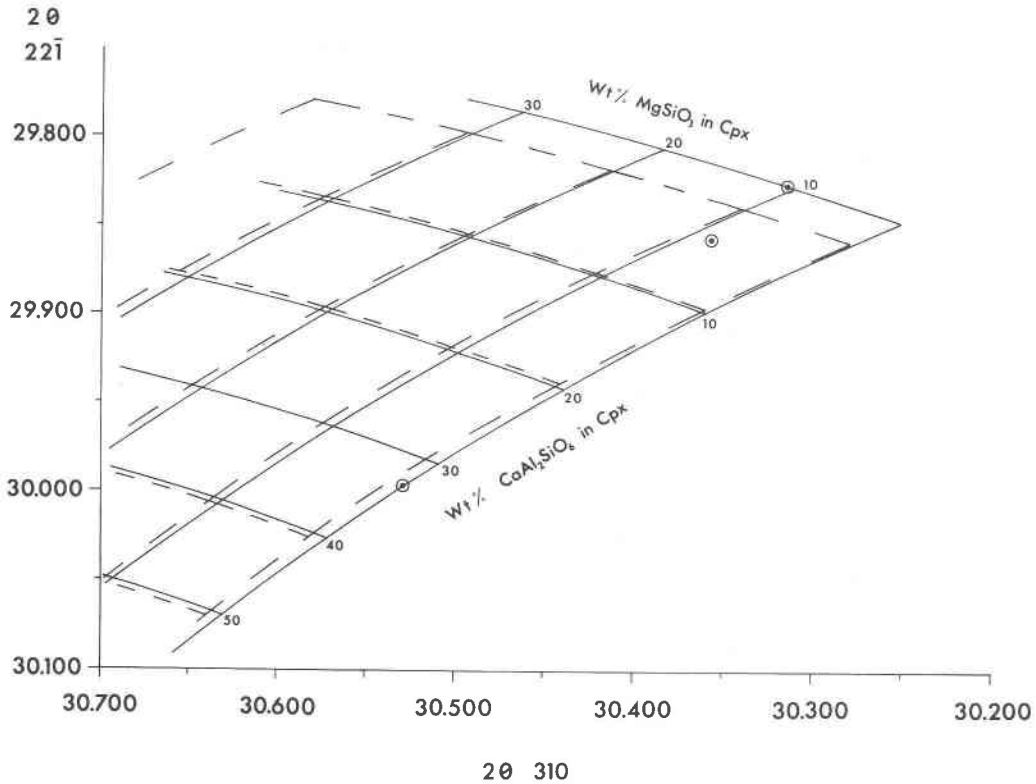

FIG. 1. Construction of the clinopyroxene composition-Cu$K\alpha$ X-ray diffraction angle grid. Circles refer to the 22$\bar{1}$ and 310 diffraction angles of three synthesized homogeneous clinopyroxenes. Explanation of broken and solid lines in the text.

can be unequivocally established. Indeed, we found no problem in reversing some of the nonequilibrated A3F charges from 1100°C to 1200°C.

Figure 3 shows that the $CaAl_2SiO_6$ content varies sympathetically with the $MgSiO_3$ content of clinopyroxene. This variation is predominantly temperature-dependent, although both pyroxene end-members decrease slightly with increasing pressure at constant temperature. Unfortunately, the parallel nature of the $CaAl_2SiO_6$ and $MgSiO_3$ isopleths of clinopyroxene in temperature–pressure space renders the composition of the mineral an indicator only of the temperature of equilibration of spinel–lherzolites. No information on the pressures of equilibration can be obtained from these data.

Application of results

The application of experimentally-determined pyroxene solid-solution variability in a simple synthetic system to the natural system has been discussed by Wood and Banno (1973) and Wood (1974). Their method of establishing simple mixing models of the solid solution phases participating in the reactions, which determine the pyroxene composition at any one temperature and pressure, will be adopted here.

In Figure 3 it was shown that the $CaAl_2SiO_6$ and $MgSiO_3$ end-members of clinopyroxene vary sympathetically with variations in temperature and pressure. This indicates that the two reactions controlling the contents of the two end-members are mutually interdependent. For simplicity, however, each reaction will be treated independently of the other.

MacGregor (1965) suggested the following reaction to account for the variations in the $CaAl_2SiO_6$ content of clinopyroxenes in spinel–peridotites with temperature and pressure:

$$\underset{\text{diopside}}{CaMgSi_2O_6} + \underset{\text{spinel}}{MgAl_2O_4} \rightleftharpoons \underset{\substack{\text{calcium}\\ \text{tschermak's}\\ \text{molecule}}}{CaAl_2SiO_6} + \underset{\text{forsterite}}{Mg_2SiO_4} \quad \Delta V = +0.96\% \qquad (1)$$

The very small positive volume change of reaction (1) is consistent with the observed small decrease in the

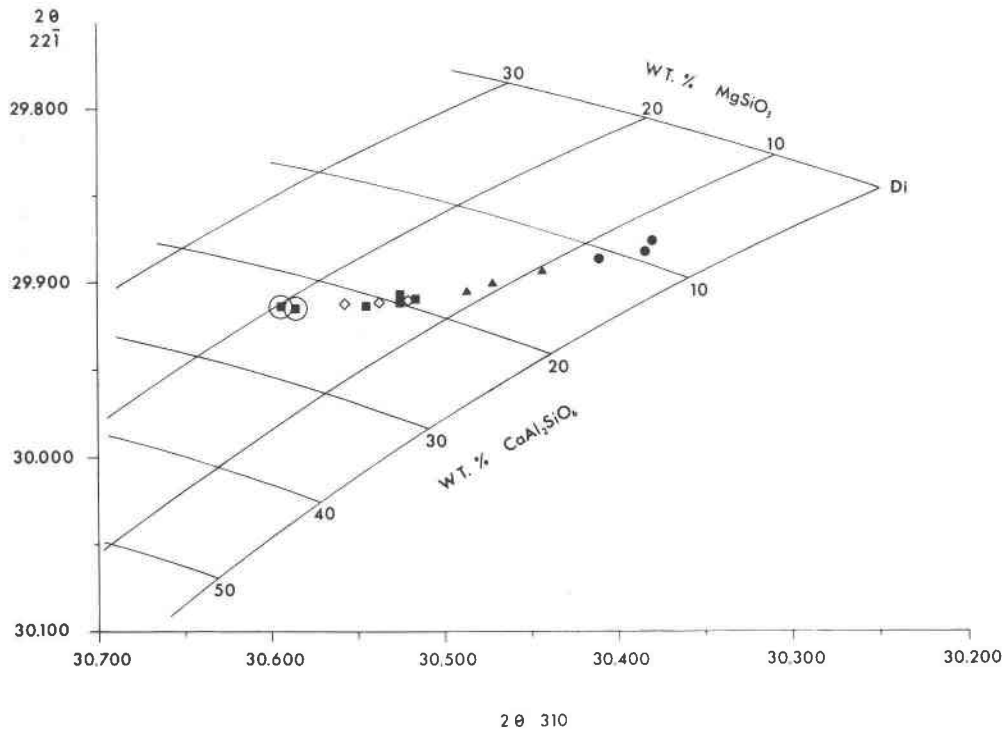

FIG. 2. 22$\bar{1}$ and 310 X-ray diffraction angles of clinopyroxenes synthesized with forsterite + orthopyroxene + spinel ± anorthite. Circles = 1100°C runs; triangles = 1200°C runs; diamonds = 1270°C runs; closed squares = 1300°C runs; squares in circles = 1400°C runs.

$CaAl_2SiO_6$ content of clinopyroxene with increasing pressure at constant temperature (Fig. 3).

The condition for equilibrium of reaction (1) is:

$$\mu\ CaMgSi_2O_6 + \mu\ MgAl_2O_4 = \mu\ CaAl_2SiO_6 + \mu\ Mg_2SiO_4 \quad (2)$$

where μ refers to the chemical potential of the component in the clinopyroxene, spinel, and olivine phases. Where the standard state of each component is the pure phase at the temperature and pressure of interest, equation (2) becomes:

$$\mu^0\ CaMg\ Si_2O_6 + RT\ \ln a\ cpx\ CaMg\ Si_2O_6 + \mu^0\ MgAl_2O_4 + RT\ \ln a\ sp\ MgAl_2O_4 = \mu^0\ CaAl_2SiO_6 + RT\ \ln a\ cpx\ CaAl_2SiO_6 + \mu^0\ Mg_2SiO_4 + RT\ \ln a\ ol\ Mg_2SiO_4 \quad (3)$$

where $RT\ln a\ y\ x$ refers to $RT\ln$ activity of component x in phase y. Rearranging (3) gives the familiar expression for equilibrium:

$$(\Delta G^0)_{T,P} = -RT\ \ln\left(\frac{a\ cpx\ CaAl_2SiO_6 \cdot a\ ol\ Mg_2SiO_4}{a\ cpx\ CaMg\ Si_2O_6 \cdot a\ sp\ MgAl_2O_4}\right) \quad (4)$$

In determining the activities of the various components in the solid phases it has been necessary to assume that the phases behave in an ideal manner. For two-site clinopyroxene solutions in which Mg^{+2}, Fe^{+2}, Ca^{+2}, Na^{+1}, and Mn^{+2} are randomly mixed in the $M2$ site, and Mg^{+2}, Fe^{+2}, Al^{+3}, Fe^{+3}, and Ti^{+4} are randomly mixed in the $M1$ site, the component activities can be approximated:

$$a\ cpx\ CaMgSi_2O_6 = X\ M2\ Ca \cdot X\ M1\ Mg \quad (5)$$

$$a\ cpx\ CaAl_2SiO_6 = X\ M2\ Ca \cdot X\ M1\ Al \quad (6)$$

where $X\ z\ i$ refers to the mole fraction of cation i in the z site. It has been shown, however, that Fe^{+2} and Mg^{+2} are not randomly distributed between the $M1$ and $M2$ sites (Hafner *et al.*, 1971; Fleet, 1974a, b). The preference of Fe^{+2} over Mg^{+2} for the $M2$ site of clinopyroxene appears most pronounced at intermediate to high mole fractions of $FeSiO_3$ (0.1 to 0.3), which are attained in clinopyroxenes of charnockites and layered igneous rocks (Fleet, 1974a, b). The clinopyroxenes of spinel–peridotites, however, commonly contain less than 0.12 mole percent $FeSiO_3$ due to high bulk Mg/Mg+Fe values of these rocks. From calculated $M1$ and $M2$ site occupancies of

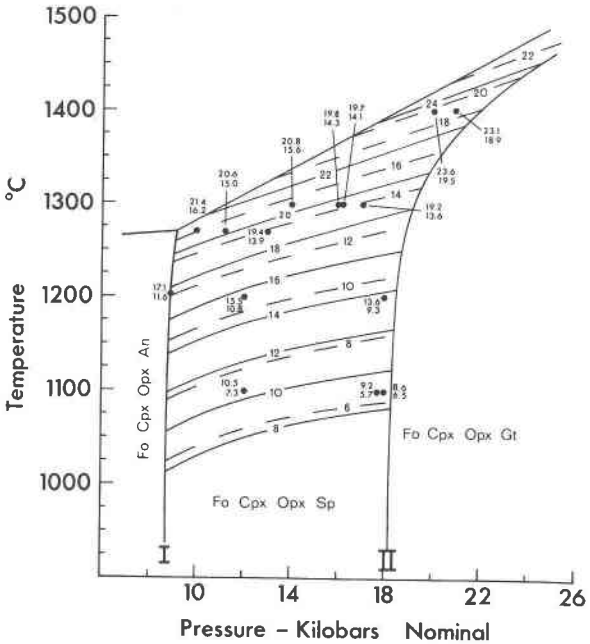

FIG. 3. Variations in the $MgSiO_3$ and $CaAl_2SiO_6$ contents of clinopyroxene with temperature and pressure in the spinel-lherzolite assemblage of the system $CaO-MgO-Al_2O_3-SiO_2$. Broken lines = $MgSiO_3$ contents in weight percent. Solid lines = $CaAlSi_2O_6$ contents in weight percent. $CaAl_2SiO_6$ value is *over* $MgSiO_3$ value for each data point. The forsterite-anorthite-clinopyroxene-orthopyroxene-spinel univariant equilibrium is shown by I (Herzberg, in preparation). The forsterite-clinopyroxene-orthopyroxene-spinel-garnet univariant equilibrium is shown by II (O'Hara *et al.*, 1971).

magnesian clinopyroxenes from the Skaergaard Intrusion (Fleet, 1974a), we have estimated that the activity of $CaMgSi_2O_6$ in clinopyroxene is about 0.03 higher than that caluclated on the basis of random Fe^{+2} distribution between the two sites. The assumption of Fe^{+2} random distribution between $M1$ and $M2$ in the particular case of the activity calculation of equation (5) does not introduce serious errors in the temperature estimation.

Because of two equivalent octahedral sites per formula unit of olivine, the activity of forsterite can be approximated:

$$a \text{ ol } Mg_2SiO_4 = (X \text{ Mg})^2 \qquad (7)$$

For normal spinels, which are the most common variety in spinel-lherzolites, the magnesium cation is located in one tetrahedral site per formula unit ($S1$), and the aluminum cations are located in two equivalent octahedral sites ($S2$). The activity of spinel proper in spinel solid solution may then be approximated:

$$a \text{ sp } MgAl_2O_4 = (X\ S1 \text{ Mg}) \cdot (X\ S2 \text{ Al})^2 \qquad (8)$$

From the 16 kbar interpolations shown in Figure 3 and from the assumption that a ol Mg_2SiO_4 and a sp $MgAl_2O_4$ were equal to one in these experiments, the relationship of

$$\ln\left(\frac{a \text{ cpx } CaAl_2SiO_6 \cdot a \text{ ol } Mg_2SiO_4}{a \text{ cpx } CaMg\,Si_2O_6 \cdot a \text{ sp } MgAl_2O_4}\right)$$

to $1/T$ (°K) was plotted and is shown in Figure 4. The experimental data fall very close to a straight line. A least-squares fit of the data in the temperature interval 1100°C to 1300°C yields the following relationship between activity ratio and temperature:

$$\ln\left(\frac{a \text{ cpx } CaAl_2SiO_6 \cdot a \text{ ol } Mg_2SiO_4}{a \text{ cpx } CaMg\,Si_2O_6 \cdot a \text{ sp } MgAl_2O_4}\right)_{16\text{ kbar}}$$

$$= \ln (K_2)_{16\text{ kbar}}$$

$$= \frac{-\Delta H^0}{RT} + \frac{\Delta S^0}{R} = \frac{-9231}{T} + 4.43 \qquad (9)$$

Where $\Delta H°$ and $\Delta S°$ refer to the standard states of the pure phases at 16 kbar and T is in °K. A least-squares fit of the 12 kbar data in the temperature interval from 1100°C to 1270°C is also shown in Figure 4 in order to illustrate the magnitude of the effect of pressure on the activity ratios. The 12 kbar data yield the following relationship:

$$\ln (K_2)_{12\text{ kbar}} = \frac{-\Delta H^0}{RT} + \frac{\Delta S^0}{R} = -\frac{8540}{T} + 4.06 \qquad (10)$$

The high $\Delta S°$ at 12 kbar (8.06cal/mole°K) and 16 kbar (8.80cal/mole°K) illustrates that this mixing model is probably an oversimplification.

Equation (10) establishes a temperature estimate of natural spinel-lherzolites based on the experimentally determined solubility of $CaAl_2SiO_6$ in clinopyroxene in the system $CaO-MgO-Al_2O_3-SiO_2$, corrected for the remaining oxide species occurring in the natural rock. This temperature estimate can be cross-checked with that estimated from the $MgSiO_3$ solubility in the same clinopyroxene crystal from the experimental data shown in Figure 3. It has been assumed that the chemical potential of $Mg_2Si_2O_6$ in clinopyroxene was equal to that of $Mg_2Si_2O_6$ in orthopyroxene for those experiments in which equilibrium is thought to have been established. The expression of this equilibrium is:

$$(\Delta G^0)_{T,P} = -RT \ln\left(\frac{a \text{ cpx } Mg_2Si_2O_6}{a \text{ opx } Mg_2Si_2O_6}\right)$$

$$= -RT \ln (K_1) \qquad (11)$$

where the relationship between activity ratio and

temperature, again assuming that both pyroxenes behave as ideal two-site solutions, may be approximated:

$$\ln (K_1) = \frac{-\Delta H^0}{RT} + \frac{\Delta S^0}{R} \qquad (12)$$

The activity of $Mg_2Si_2O_6$ in clinopyroxene can be estimated from Figure 3 and is approximated by the expression:

$$a \text{ cpx } Mg_2Si_2O_6 = X\,M2\text{ Ca} \cdot X\,M1\text{ Mg} \qquad (13)$$

An approximation of the activity of $Mg_2Si_2O_6$ in orthopyroxene is given by the following expression:

$$a \text{ opx } Mg_2Si_2O_6 = X\,M2\text{ Mg} \cdot X\,M1\text{ Mg} \qquad (14)$$

Because no data on orthopyroxene compositions were obtained in this study, the activity of $Mg_2Si_2O_6$ in orthopyroxene in the spinel–lherzolite assemblage was estimated from available experimental data. The mole fraction of magnesium in the $M2$ site of orthopyroxene at 12 and 16 kbar was taken from experimentally derived values of diopside solubility in orthopyroxene coexisting with clinopyroxene in the system $CaO–MgO–SiO_2$ (Mori and Green, 1975). The similarity of the results of Akella (1974) with those of Nehru and Wyllie (1974) and Mori and Green (1975) suggests that the presence of an aluminous phase in equilibrium with clinopyroxene and orthopyroxene does not appreciably affect the diopside solubility in orthopyroxene. The mole fraction of magnesium in the $M1$ site of orthopyroxene was estimated from the assumption that ($X\,M1$ Al)opx = ($X\,M1$ Al)cpx in the spinel–lherzolite assemblage at the same temperature and pressure.

In Figure 4 the relationship of $\ln K_1$ *vs.* $1/T$ at 12 and 16 kbar is also plotted. Least-squares fits of the data yield the following expressions:

$$\ln (K_1)_{12\text{kbar}} = \frac{-8392}{T} + 3.64 \qquad (16)$$

and

$$\ln (K_1)_{16\text{kbar}} = \frac{-8494}{T} + 3.58 \qquad (17)$$

where $\Delta S°$ at 12 kbar and 16 kbar are 7.25cal/mole°K and 7.12cal/mole°K respectively. These values of the entropy change for the transfer of $Mg_2Si_2O_6$ from orthopyroxene to clinopyroxene are lower than that for the 30 kbar Davis and Boyd (1966) results (10.63cal/mole°K), but they are higher than those for the 10 and 30 kbar Mori and Green (1975) results (5.60 and 5.66cal/mole°K respectively) and the Nehru and Wyllie (1974) 30 kbar results in

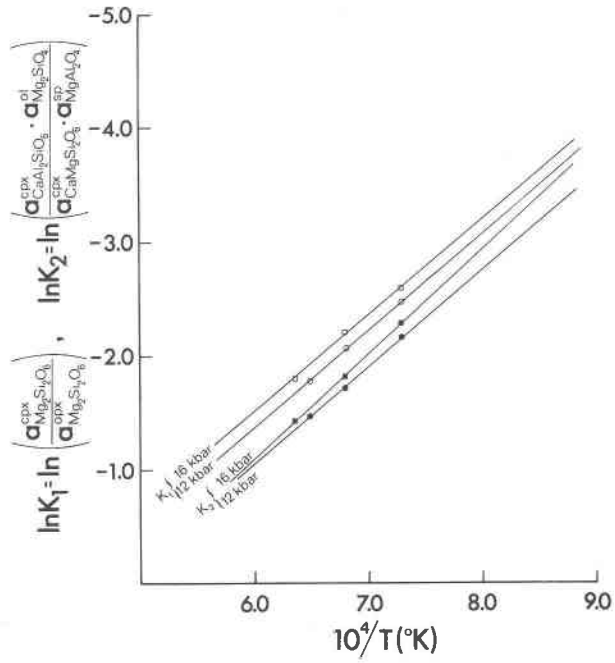

FIG. 4. Plot of ln $(a^{cpx}_{Mg_2Si_2O_6}/a^{opx}_{Mg_2Si_2O_6})$ and ln $(a^{cpx}_{CaAl_2SiO_6} \cdot a^{ol}_{Mg_2SiO_4}/a^{cpx}_{CaMgSi_2O_6} \cdot a^{sp}_{MgAl_2O_4})$ *vs.* $1/T$ for coexisting phases of the spinel–lherzolite assemblage in the system $CaO–MgO–Al_2O_3–SiO_2$.

the interval 1000°C to 1500°C(5.32cal/mole°K). All of these entropy change values, which are probably too high, testify to the simplicity of the ideal solid-solution models. The values at 12 kbar and 16 kbar from this work may differ from the Mori and Green results because of the presence of Al_2O_3 in the system of this work, differences in analytical technique, or because of the assumptions used in estimating the activity of $Mg_2Si_2O_6$ in orthopyroxene. It is significant to note that at any given temperature, the solubility of $Mg_2Si_2O_6$ in clinopyroxene noted from our experiments in the alumina-bearing system at 12 kbar is considerably less than that from the experiments of Mori and Green in the alumina-free system at 10 kbars. The solubility difference is such that the temperature estimated from any one value of K_1 from our data may be up to 150°C higher than that estimated from the Mori and Green data.

Estimation of equilibrium temperatures

Using published and available unpublished mineral analyses of coexisting olivine, clinopyroxene, orthopyroxene, and spinel phases from spinel–lherzolites from alpine-type intrusions and nodules in basalts, temperature estimations have been made from the calculated values of K_1 and K_2 at 12 and 16 kbar.

The calculations of the activities of $CaAl_2SiO_6$,

$CaMgSi_2O_6$, and $Mg_2Si_2O_6$ in the natural clinopyroxenes were simplified by calculating first the ferrous-ferric proportions as presented by Mysen and Heier (1972) (for those analyses where Fe_2O_3 was not determined), and second the pyroxene end-member molecules as proposed by Kushiro (1962) and Cawthorn and Collerson (1974). A breakdown of each clinopyroxene analysis into its end-members provided a simple method of estimating *X M*2 Ca, *X M*1 Al, and *X M*1 Mg independently of the silicon analysis. Wood and Banno (1973) discussed the alternative methods of establishing *a* cpx $Mg_2Si_2O_6$/*a* opx $Mg_2Si_2O_6$ that may be used to correct for the marked increase in the orthopyroxene (enstatite + ferrosilite) solubility in clinopyroxene with increasing Fe^{+2} in the system. Fortunately, this is not a serious problem in the natural spinel–lherzolite system because of low amounts of ferrosilite in clinopyroxene. However, the correction scheme that was adopted here involved projecting the clinopyroxene analysis from ferrosilite to the remaining pyroxene end-members. The method of calculating *a* opx $Mg_2Si_2O_6$ used here was described by Wood (1974).

The calculated temperatures are given in Table 2. Figure 5 shows the frequency distribution of the K_1 and K_2 temperature estimations for alpine-type intrusions, nodules in basalts, and the two spinel-lherzolite occurrences together. The important points which emerge from this treatment of the data are:

(1) The mean of 38 K_2 temperatures and the standard deviation for *both* occurrences is 1193°C (*i.e.* about 50°C below the anhydrous peridotite solidus) and 94°C, respectively. The mean K_2 temperature for the 23 nodule analyses is 1194°C, and the standard deviation is 75°C. The mean K_2 temperature for the 15 intrusion analyses is 1190°C, and the standard deviation is 188°C. Whereas the means are essentially the same for both occurrences, there is a greater spread of K_2 intrusion temperatures. The highest frequency of K_2 nodule temperatures coincides with the anhydrous solidus temperature, whereas the highest frequency of the K_2 intrusion temperatures lies between the anhydrous solidus and the solidus with a water content of 0.2 percent. Most K_2 temperatures are between those of the two solidii.

(2) The mean of 43 K_1 temperatures and the standard deviation for both peridotite occurrences is 1095°C and 131°C, respectively. For the nodules the mean of 23 K_1 temperatures is 1151°C, and the standard deviation is 100°C. For the intrusions the mean of 20 K_1 temperatures is 1030°C, and the standard deviation is 132°C. Again note the greater spread of K_1 intrusion temperatures. The highest frequency of K_1 nodule temperatures is between the two solidii, and the mean is within 40°C of the mean K_2 nodule temperatures. The mean and highest frequency of K_1 intrusion temperatures, however, are much lower (<150°C) than those of the K_2 intrusion temperatures.

At pressures greater than 12 kbar but within the spinel–lherzolite stability field (O'Hara *et al.*, 1971), the relationships between the solidii, the mean K_1 and K_2 temperatures of the nodules and intrusion, and the degree of incongruity between the K_1 and K_2 temperatures are similar to those discussed at 12 kbar.

With the exception of the Scourian spinel-lherzolite, which has clearly been recrystallized under granulite facies conditions (O'Hara, 1961), the remainder of the nodules and intrusions crystallized from solidus temperature conditions without substantial intercrystalline cationic reequilibration to temperatures along normal suboceanic or subcontinental mantle geothermal gradients (Ringwood, 1966). We would like to present for consideration a hypothesis which may explain the incongruous nature of the K_1 and K_2 temperature estimations in terms of variable cooling rates from solidus temperatures, the rates of which determine the extent to which chemical reequilibration can be attained at all stages in the cooling history. If the rate of exchange of $Mg_2Si_2O_6$ from clinopyroxene to orthopyroxene is greater than that for the reaction of aluminous clinopyroxene with olivine to produce a less aluminous clinopyroxene and spinel, then K_1 quenching temperatures should be consistently lower than K_2 quenching temperatures during rapid cooling of the intrusions from solidus temperatures to cooler lower crustal or upper mantle temperatures. These data suggest that solidus K_2 temperatures were quenched, whereas K_1 temperatures tended to partially reequilibrate to subsolidus temperatures. The greater degree of congruity and the lesser statistical spread of K_1 and K_2 temperatures of the nodules in basalt suggest that little time for partial K_1 reequilibration to subsolidus temperatures may have been available prior to quenching by eruption to the surface; a condition indicating a close genetic relationship between the nodules and the volcanic activity.

The possibility of differential reequilibration rates between the K_1 and K_2 equilibria is best illustrated by the southwestern Oregon spinel–lherzolites (Medaris, 1972). K_1 temperatures calculated for the coexisting primary augen and recrystallized matrix pyroxenes are all similar (966°C to 1031°C) and lower than the

TABLE 2. Activities, equilibrium constants, and temperature estimations of spinel-lherzolites

References	Specimen	$a^{cpx}_{CaAl_2SiO_6}$	$a^{cpx}_{CaMgSi_2O_6}$	$a^{cpx}_{Mg_2Si_2O_6}$	$a^{opx}_{Mg_2Si_2O_6}$	$a^{ol}_{Mg_2SiO_4}$	$a^{sp}_{MgAl_2O_4}$	$\ln K_1$	$\ln K_2$	$T(K_1)_{12kbar}$ °C	$T(K_2)_{12kbar}$ °C	$T(K_1)_{16kbar}$ °C	$T(K_2)_{16kbar}$ °C
INTRUSIONS													
1	90683	0.105	0.598	0.106	0.638	0.766	0.442	-1.795	-1.190	1268	1351	1306	1368
1	90681	0.101	0.615	0.133	0.638	0.778	0.434	-1.568	-1.223	1334	1341	1375	1358
2	x282	-	-	0.014	0.591	-	-	-3.743	-	866	-	886	-
3	37,310	-	-	0.029	0.612	-	-	-3.049	-	982	-	1008	-
4	-	0.055	0.607	0.041	0.781	0.775	0.673	-2.947	-2.260	1002	1077	1028	1105
5	-	0.040	0.603	0.037	0.752	0.813	0.643	-3.012	-2.478	990	1032	1015	1062
6	M5-186	-	-	0.016	0.700	-	-	-3.778	-	861	-	881	-
6	M6-128	-	-	0.075	0.673	-	-	-2.194	-	1164	-	1197	-
7	VH-Augen	0.064	0.675	0.036	0.696	0.810	0.556	-2.965	-1.979	999	1139	1024	1166
7	VH-Matrix	0.040	0.685	0.033	0.762	0.810	0.556	-3.139	-2.464	966	1034	990	1065
7	C-Augen	0.075	0.754	0.043	0.705	0.810	0.559	-2.797	-1.516	1031	1256	1058	1278
7	C-Matrix	0.064	0.769	0.043	0.738	0.810	0.559	-2.843	-2.115	1022	1108	1049	1136
7	SB-Augen	0.069	0.733	0.039	0.738	0.812	0.478	-2.940	-1.833	1003	1174	1029	1199
7	SB-Matrix	0.054	0.760	0.044	0.764	0.812	0.478	-2.854	-2.114	1020	1108	1046	1136
7	SC	0.075	0.798	0.043	0.751	0.819	0.277	-2.860	-0.881	1019	1452	1045	1463
8	3	0.097	0.715	0.009	0.700	0.798	0.517	-4.321	-1.560	784	1244	801	1267
8	7	0.071	0.698	0.040	0.733	0.824	0.423	-2.906	-1.617	1009	1229	1035	1251
8	10	0.094	0.719	0.025	0.704	0.797	0.676	-3.334	-1.874	931	1164	956	1189
9	B3	0.059	0.596	0.063	0.659	0.824	0.588	-2.352	-1.974	1125	1139	1159	1167
9	B38	0.074	0.579	0.095	0.678	0.825	-	-1.961	-	1224	-	1261	-
NODULES													
10	R375	0.069	0.599	0.105	0.701	0.769	0.513	-1.899	-1.756	1240	1193	1276	1218
10	R376	0.071	0.614	0.090	0.679	0.774	0.507	-2.021	-1.734	1207	1199	1242	1223
11	E-1	0.057	0.658	0.025	0.747	0.805	0.641	-3.397	-2.218	922	1086	944	1114
12	C.H.	0.051	0.590	0.157	0.739	0.807	0.414	-1.549	-1.781	1340	1187	1382	1212
13	6/40	0.059	0.620	0.090	0.702	0.796	0.505	-2.054	-1.897	1199	1158	1234	1185
14	1	0.076	0.632	0.061	0.740	0.808	0.566	-2.496	-1.764	1094	1191	1124	1216
14	2	0.072	0.549	0.112	0.708	0.797	0.570	-1.844	-1.700	1254	1208	1292	1231
14	4	0.088	0.603	0.058	0.669	0.801	0.620	-2.445	-1.668	1106	1210	1136	1239
14	7	0.072	0.563	0.097	0.696	0.785	0.510	-1.971	-1.625	1220	1227	1256	1250
14	8	0.086	0.639	0.061	0.713	0.809	0.521	-2.459	-1.566	1103	1243	1133	1265
14	9	0.090	0.651	0.042	0.717	0.791	0.584	-2.837	-1.675	1024	1214	1050	1238
14	10	0.079	0.612	0.066	0.775	0.791	0.510	-2.478	-1.608	1098	1231	1128	1254
15	2604	0.027	0.683	0.076	0.775	0.833	0.337	-2.348	-2.326	1128	1063	1159	1092
15	2669	0.054	0.654	0.078	0.791	0.823	0.618	-2.317	-2.208	1135	1088	1166	1116
15	2640	0.058	0.537	0.101	0.716	0.762	0.324	-1.959	-1.370	1224	1297	1259	1317
15	2728	0.051	0.623	0.044	0.753	0.818	0.513	-2.840	-2.036	1024	1126	1049	1153
15	2700	0.047	0.586	0.073	0.735	0.798	0.272	-2.309	-1.447	1137	1275	1168	1296
15	2642	0.057	0.700	0.041	0.740	0.809	0.612	-2.893	-2.229	1013	1083	1038	1112
16	1	0.078	0.617	0.078	0.726	0.818	0.441	-2.231	-1.450	1155	1275	1188	1295
16	4	0.077	0.518	0.147	0.679	0.808	0.470	-1.530	-1.364	1346	1299	1388	1319
16	2	0.076	0.573	0.084	0.700	0.810	0.372	-2.120	-1.242	1182	1335	1216	1352
16	7	0.074	0.676	0.062	0.718	0.788	0.511	-2.449	-1.779	1105	1187	1135	1212
17	38	0.007	0.712	0.101	0.727	0.820	0.072	-1.974	-2.190	1220	1092	1255	1120

INTRUSIONS: 1=Lizard;Green (1964). 2=Scourie;O'Hara (1961). 3=Scourie;Muir and Tilley (1958). 4=Etang de Lherz;O'Hara et al. (1971). 5=Etang de Lherz;Hunter (unpublished). 6=Beni Bouchera;Kornprobst (1969). 7=Oregon;Medaris (1972). 8=Hare Bay, Bay of Islands, Newfoundland;Riccio (1976). 9=Baldissero;Etienne (1971).

NODULES: 10=Austria;Richter (1971). 11=Fife,Scotland;Chapman (1976). 12=Derbyshire;Hamad (1963). 13=Russia;Kutolin and Frolova (1970). 14=Norway;Griffin (1973). 15=Victoria, Australia;Frey and Green (1974). 16=various localities;Ross et al. (1954). 17=Hawaii; Kuno (1969).

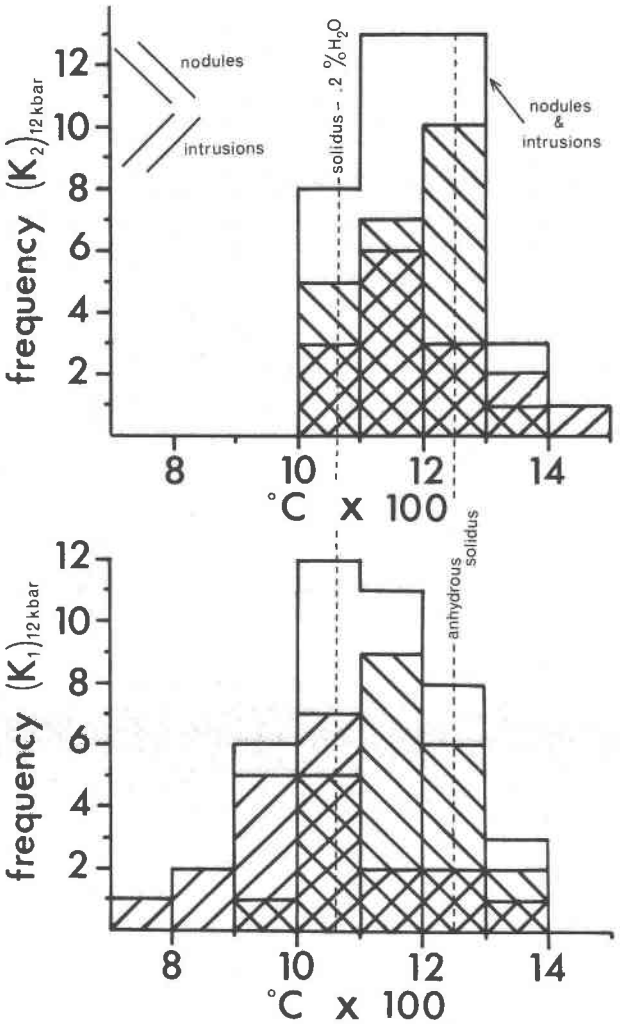

FIG. 5. Histograms of temperature estimations of spinel-lherzolites from alpine-type peridotites and nodules in basalt. Explanation of the K_1 and K_2 equilibrium constants in the text. Anhydrous peridotite solidus from Kornprobst (1970) and Green and Ringwood (1967). Water-undersaturated (0.2%) peridotite solidus from Millhollen *et al.* (1974).

K_2 temperatures by 68°C to 225°C. K_2 temperatures from the augen clinopyroxenes are at least 100°C higher than K_2 temperatures from the recrystallized matrix clinopyroxenes. A correlation is apparent between the degree of subsolidus recrystallization, which is reflected texturally by the degree of grain-size reduction, and the temperatures indicated by the K_2 equilibrium, which are reflected chemically by the alumina contents of the pyroxenes.

We realize the limitations of any hypothesis generated from the utilization of analyses in the literature. It is hoped, however, that the geological implications of these experimental data will stimulate future detailed studies on the textural and geochemical interrelationships of spinel-lherzolites. Special attention must now be placed upon the textural control of the chemistry of coexisting solid solution phases, the chemical homogeneity (or heterogeneity) within any one crystal, and the variations in the mineral chemistry from one location of an intrusion to another or one textural class of nodules to another (Mercier and Nicolas, 1975). The kinetic problems discussed pose the necessity of establishing equilibrium before any temperature estimations become geologically meaningful.

Conclusions

Experiments in the system $CaO-MgO-Al_2O_3-SiO_2$ have shown that the $CaAl_2SiO_6$ content of clinopyroxenes in the spinel-lherzolite assemblage varies sympathetically with the $MgSiO_3$ content with variations in temperature and pressure. Such variations are predominantly temperature-dependent, although both pyroxene end-members decrease slightly in amount with increasing pressure at constant temperature. Contrary to O'Hara (1967), the isopleths of $CaAl_2SiO_6$ and $MgSiO_3$ of clinopyroxene in temperature–pressure space were found to be parallel, rendering these two pyroxene molecules indicators only of the temperature of equilibrium of spinel-lherzolites. No information on the pressures of equilibration can be obtained. A comparison of these results with those of Mori and Green (1975) in the system $CaO-MgO-SiO_2$ suggests that the activity of $Mg_2Si_2O_6$ in clinopyroxene is considerably reduced with increasing activity of $CaAl_2SiO_6$ at any one temperature and pressure. Temperatures of equilibration of spinel-lherzolites determined from experimental data of the diopside–enstatite solvus in the alumina-free system may be up to 150°C too low.

From these experimental data and by using simple ideal mixing models of the solid solution phases participating in the exchange reactions, two temperature estimates were made on spinel-lherzolites from nodules in basalts and alpine-type intrusions. The temperatures indicated by the alumina and enstatite contents of the clinopyroxenes in the spinel-lherzolite nodules range from those of the anhydrous peridotite solidus to those of the water-undersaturated peridotite solidus. No subsolidus reequilibration took place, suggesting a close genetic relationship between the nodules and either the host basalts or the basalts of the same fractionation suite. The temperatures estimated by the alumina contents of the clinopyroxenes in the spinel-lherzolite intrusions, which have not

been affected by post-intrusion metamorphism, also indicate solidus temperatures. However, the temperatures indicated by the $MgSiO_3$ contents of the same clinopyroxenes of these intrusions range from the anhydrous solidus to several hundred degrees in the subsolidus. These incongruous temperatures are attributed to differential intercrystalline cationic exchange rates between the reaction governing the enstatite content and the reaction governing the alumina content of the clinopyroxene. In view of the low subsolidus reequilibration rates the subsolidus temperatures may bear no relation to the temperatures of a geotherm (MacGregor, 1974; MacGregor and Basu, 1974); indeed, they may only represent a 'quench' temperature below which further reequilibration became retarded in the absence of metamorphic reworking. In contrast to 'thermally quiescent' deeper-level garnet-lherzolites, which appear to have been in chemical equilibrium along normal subcontinental mantle geothermal gradients (Boyd, 1973; Boyd and Nixon, 1973; Carswell, 1974), most spinel-lherzolites appear to be the vestiges of complex mantle thermal perturbations and/or partial melting events.

Acknowledgments

This work was supported by an Edinburgh University Studentship and a National Research Council of Canada postgraduate scholarship. We are grateful to Professor M. J. O'Hara who kindly provided the experimental facilities and useful criticisms during the research period of the senior author at the Grant Institute of Geology, Edinburgh, Scotland.

References

AKELLA, J. (1974) Solubility of Al_2O_3 in orthopyroxene coexisting with garnet and clinopyroxene for compositions on the diopside–pyrope join in the system $CaSiO_3$–$MgSiO_3$–Al_2O_3. *Carnegie Inst. Wash. Year Book,* **73,** 273–278.

BIGGAR, G. M. (1969) The isothermal, isobaric subsolidus diopside solid solution volume in the system CaO–MgO–Al_2O_3–SiO_2. *Progress in Experimental Petrology 1,* Natural Environmental Research Council Publications Series D, London, 97–104.

——— AND M. J. O'HARA (1969) A comparison of gel and glass starting materials for phase equilibrium studies. *Mineral. Mag.* **37,** 198–205.

BOYD, F. R. (1973) A pyroxene geotherm. *Geochim. Cosmochim. Acta,* **37,** 2533–2546.

——— AND P. H. NIXON (1973) Structure of the upper mantle beneath Lesotho. *Carnegie Inst. Wash. Year Book,* **72,** 431–445.

CARSWELL, D. A. (1974) Comparative equilibration temperatures and pressures of garnet lherzolites in Norwegian gneisses and in kimberlite. *Lithos,* **7,** 113–12.

CAWTHORN, R. G. AND K. D. COLLERSON (1974) The recalculation of pyroxene end-member parameters and the estimation of ferrous and ferric iron content from electron microprobe analyses. *Am. Mineral.* **59,** 1203–1208.

CHAPMAN, N. A. (1976) Inclusions and megacrysts from undersaturated tuffs and basanites, East Fife, Scotland. *J. Petrol.* in press.

CLARK, S. P., J. F. SCHAIRER AND J. DE NEUFVILLE (1962) Phase relations in the system $CaMgSi_2O_6$–$CaAl_2SiO_6$–SiO_2 at low and high pressure. *Carnegie Inst. Wash. Yearbook,* **61,** 59–68.

DAVIS, B. T. C. AND F. R. BOYD (1966) The join $Mg_2Si_2O_6$–$CaMgSi_2O_6$ at 30 kb and its application to pyroxenes from kimberlite. *J. Geophys. Res.* **71,** 3567–3576.

ETIENNE, F. (1971) *La lherzolite rubanée de Baldissero Canavese.* Ph.D. thesis, University of Nantes.

FLEET, M. E. (1974a) Partition of Mg and Fe^{2+} in coexisting pyroxenes. *Contrib. Mineral. Petrol.* **44,** 251–257.

——— (1974b) Mg, Fe^{2+} site occupancies in coexisting pyroxenes. *Contrib. Mineral. Petrol.* **47,** 207–214.

FREY, F. A. AND D. H. GREEN (1974) The mineralogy, geochemistry and origin of lherzolite inclusions in Victorian basanites. *Geochim. Cosmochim. Acta,* **38,** 1023–1059.

GREEN, D. H. (1964) The petrogenesis of the high-temperature peridotite intrusion in the Lizard area, Cornwall. *J. Petrol.* **5,** 134–188.

——— AND A. E. RINGWOOD (1967) The stability fields of aluminous pyroxene peridotite and garnet peridotite and their relevance in upper mantle structure. *Earth Planet. Sci. Lett.* **3,** 151–160.

GRIFFIN, W. L. (1973) Lherzolite nodules from the Fen Alkaline Complex, Norway. *Contrib. Mineral. Petrol.* **38,** 135–146.

HAFNER, S. S., D. VIRGO AND D. WARBURTON (1971) Cation distributions and cooling history of clinopyroxenes from Oceanus Procellarum. *Proc. 2nd Lunar Sci. Conf.* **1,** 99–108.

HAMAD, S. EL D. (1963) The chemistry and mineralogy of the olivine nodules of Calton Hill, Derbyshire. *Mineral. Mag.* **33,** 483–497.

HOWELLS, S. AND M. J. O'HARA (1975) Paleogeotherms and the diopside–enstatite solvus. *Nature,* **254,** 406–408.

KORNPROBST, J. (1969) Le massif ultrabasique des Beni Bouchera (Rif Interne, Moroc): Etude des péridotites de haute température et de haute pression, et des pyroxénolites, à grenat ou sans grenat, qui leur sont associees. *Contrib. Mineral. Petrol.* **23,** 283–322.

——— (1970) Les peridotites et les pyroxenolites du massif ultrabasique des Beni Bouchera: une etude experimentale entre 1100 et 1550°C, sous 15 a 30 kilobars de pression seche. *Contrib. Mineral. Petrol.* **29,** 290–309.

KUNO, H. (1969) Mafic and ultramafic nodules in basaltic rocks of Hawaii. *Geol. Soc. Am. Mem.* **115,** 189–234.

KUSHIRO, I. (1962) Clinopyroxene solid solutions. Part 1. The $CaAl_2SiO_6$ component. *Japan J. Geol. Geogr.* **33,** 213–220.

KUTOLIN, V. A. AND V. M. FROLOVA (1970) Petrography of ultrabasic inclusions from basalts of Minusa and Transbaikalian Regions. *Contrib. Mineral. Petrol.* **29,** 163–179.

MACGREGOR, I. D. (1965) Aluminous diopsides in the three-part assemblage diopside solid solution + forsterite + spinel. *Carnegie Inst. Wash. Year Book,* **64,** 134–135.

——— (1974) The system MgO–Al_2O_3–SiO_2: Solubility of Al_2O_3 in enstatite for spinel and garnet peridotite compositions. *Am. Mineral.* **59,** 110–119.

——— AND A. R. BASU (1974) Thermal structure of the lithosphere: a petrologic model. *Science,* **185,** 1007–1011.

MEDARIS, L. G., JR. (1972) High-pressure peridotites in southwestern Oregon. *Geol. Soc. Am. Bull.* **83,** 41–58.

MERCIER, J-C. C. AND A. NICOLAS (1975) Textures and fabrics of

upper mantle peridotites as illustrated by xenoliths from basalts. *J. Petrol.* **16,** 454–487.

MILLHOLLEN, G. L., A. J. IRVING AND P. J. WYLLIE (1974) Melting interval of peridotite with 5.7 percent water to 30 kilobars. *J. Geol.* **82,** 575–587.

MORI, T. AND D. H. GREEN (1975) Pyroxenes in the system $Mg_2Si_2O_6$–$CaMgSi_2O_6$ at high pressure. *Earth Planet. Sci. Lett.* **26,** 277–286.

MUIR, I. D. AND C. E. TILLEY (1958) The composition of coexisting pyroxenes in metamorphic assemblages. *Geol. Mag.* **95,** 403–409.

MYSEN, B. O. AND K. S. HEIER (1972) Petrogenesis of eclogites in high grade metamorphic gneisses, exemplified by the Hareidland eclogite, western Norway. *Contrib. Mineral. Petrol.* **36,** 73–94.

NEHRU, C. E. AND P. J. WYLLIE (1974) Electron microprobe measurement of pyroxenes coexisting with H_2O-undersaturated liquid in the join $CaMgSi_2O_6$–$Mg_2Si_2O_6$–H_2O at 30 kilobars, with applications to geothermometry. *Contrib. Mineral. Petrol.* **48,** 221–228.

O'HARA, M. J. (1961) Zoned basic and ultrabasic gneiss masses in the early Lewisian metamorphic complex at Scourie, Sutherland. *J. Petrol.* **2,** 248–276.

——— (1967) Mineral parageneses in ultrabasic rocks. In, *Ultramafic and Related Rocks.* John Wiley and Sons, Inc., New York. p. 393–401.

——— S. W. RICHARDSON AND G. WILSON (1971) Garnet peridotite stability and occurrence in crust and mantle. *Contrib. Mineral. Petrol.* **32,** 48–68.

——— AND J. F. SCHAIRER (1963) The join diopside-pyrope at atmospheric pressure. *Carnegie Inst. Wash. Year Book,* **62,** 107–115.

RICCIO, L. (1976) *Stratigraphy and petrology of the peridotite–gabbro component of the western Newfoundland ophiolites.* Ph.D. thesis, University of Western Ontario.

RICHARDSON, S. W., P. M. BELL AND M. C. GILBERT (1968) Kyanite–sillimanite equilibrium between 700°C and 1500°C. *Am. J. Sci.* **266,** 513–541.

RICHTER, W. (1971) Ariégite, Spinell-Peridotite und Phlogopit-Klinopyroxenite aus dem Tuff von Tobaj im südlichen Burgenland. *Tschermaks Mineral. Petrol. Mitt.* **16,** 227–251.

RINGWOOD, A. E. (1966) Mineralogy of the mantle. In, P. M. Hurley, *Advances in Earth Sciences.* M.I.T. Press, Cambridge, Massachusetts, 357–399.

ROSS, C. S., M. D. FOSTER AND A. T. MYERS (1954) Origin of dunites and of olivine-rich inclusions in basaltic rocks. *Am. Mineral.* **39,** 693–737.

WOOD, B. J. (1974) The solubility of alumina in orthopyroxene coexisting with garnet. *Contrib. Mineral. Petrol.* **46,** 1–15.

——— AND S. BANNO (1973) Garnet–orthopyroxene and orthopyroxene–clinopyroxene relationships in simple and complex systems. *Contrib. Mineral. Petrol.* **42,** 109–124.